Development and biomedical application of nanocomposites: *in situ* fabrication of ZnO–PbO nanocomposite through microwave method

A. Rajabi, M. Aieneravaie, V. Dorosti and S. K. Sadrnezhaad*

A novel nanocomposite of ZnO–PbO with flower-like nanostructure was fabricated from zinc acetate and lead nitrate as principle raw materials via an in situ process. The novelty of this study consists in the use of a common approach for fabricating of ZnO and PbO nanoparticles simultaneously. From these experiments the conclusion might be drawn that $Zn(NH_4)_2^{4+}$ ions and $Pb(OH)_2$ act as precursors for the nucleation and growth of ZnO and PbO respectively under microwave irradiation. The precursors formation were carried at two stages: reaction between zinc ions and lead nitrate with ammonium ion and hydroxide sodium respectively. The average crystalline size of Zno and PbO has been analysed by X-ray diffraction (XRD) pattern and estimated to be 43·5 and 54·5 nm for ZnO and PbO respectively. Brunauer–Emmet–Teller (BET-N_2) analyses of as prepared material demonstrated that this nanostructure material has a high specific surface area, as high as 150 $m^2\ g^{-1}$ which can be promising targets for adsorbent materials. The Formation mechanism of ZnO–Pbo nanocomposite is also studied.

Keywords: Nanocomposite, ZnO–PbO, Microwave method

Introduction

Expansion of knowledge has been witnessed in various fields of sciences and technology; however, remarkable advances still appear through more recent fields namely nanotechnology. Although the appearance of nanoscience can be related to the nineteenth century field of collide chemistry, the primary studies has commenced since 1980s and are still significantly developing at a fast rate.[1,2]

With the quick development of nanotechnology, nanocomposites have demonstrated better mechanical properties than conventional composites which are made of micrometre size components.[3] It is worth noting, nanocomposites composed of a multiphase which one of the phases is in the nanocrystalline regime. Indeed, it can generally improve composite mechanical properties.[4] Accordingly, due to various applications in industries, nanocomposites based on nanooxide have been considerably studied. It can be related to the unique properties of metal oxides are used in the fabrication of microelectronic circuits,[5] thermo electronic,[6] semiconductors,[7] sensors,[8] pigments,[9] photo electronic properties,[10] fuel cells and optic thermo electronic.[11] Among nanooxides, Zinc oxide and Lead oxide have been more popular with scholars, since Zinc oxide is a sufficient candidate for making catalysts,[12] solar cells,[13] ultraviolet protection films,[14] electromagnetic detectors and piezoelectric.[15–17]

Using chemotherapeutic drugs can control growth rate of tumors. However, because of toxic substance a fair assessment of this method is still a difficult issue. Efforts are made to be able to reduce this problem through tumor targeting drug delivery system. In order to achieve the objective, ZnO or ZnS based materials have been recently synthesised for quantum dot which can be biofriendly candidate for biological technology application. Moreover, photoluminescent semiconductor quantum dots (QDs) have gained considerable attention as biological labels, fluorescent and bioimaging and fluorescence labelling. In this regard, embedding of ZnO QDs on silica nanospheres results in significant increase in photoluminescence intensity.[18] Recently, it has been reported that nano ZnO QDS on Si nanospheres can be a good candidate for tracking cancer cells in cell therapy.[19] The doping nano ZnO with low concentration of Mn^{+2} increases the luminescence and band-gap energy ZnO. Therefore, drug loaded chitosan encapsulated ZnO:Mn^{+2} QDs can be utilised as deliver tumour targeted drugs.[20] Another relevant study was achieved by Chandrasekaran *et Al.*[21] who synthesised ZnS(Cd) nanorod for drug carrier and bioimaging.

Also, it has been found that Lead oxide is utilised for gas sensors,[8] and storage batteries as specialised

Department of Materials Science and Engineering, Centre of Excellence for Production of Advanced Materials, Sharif University of Technology, Tehran, Iran

*Corresponding author, email nanomaterialgroup@hotmail.com

Received 25 January 2014; accepted 28 February 2014
DOI 10.1179/1753555714Y.0000000138

material.[22,23] Furthermore, nano PbO improves sintered density, electrical resistivity and permeability.[24]

Although, nanomaterials can be produced by several methods including, mechanical alloying,[25] disintegrated melt deposition (DMD),[26] sol–gel reaction,[27] hydrothermal process,[28] thermal evaporation,[29] chemical vapour deposition,[30] and solution growth process.[31] There are a number of malfunctions for the synthesis of nanocomposites. The most notable problems in this regard are those related to the requirement of expensive and advanced equipment as well as complexities of controlling procedure.[32,33] Previous studies have showed that the usage of microwave heating for chemical synthesis has sharply increased in recent decades due to fast synthesis, low cost, simple process and reliability.[34,35]

Notwithstanding, extensive investigations have been performed in the field of nanotechnology, ZnO–PbO nanocomposite has not been simultaneously prepared yet. Therefore, the present authors were persuaded to make ZnO–PbO nanocomposite through thermal decomposition technique by microwave due to simplicity, fastness and cheapness. It is well conceived that adequate data is not available for physical–chemical properties of ZnO–PbO nanocomposite. Hence, this study can hopefully generate an opportunity for other researchers to fill this gap.

Experimental

All the raw materials were of analytical grade and were purchased from Merck, Germany. A primary solution was prepared by adding 25 mL ammonium hydroxide (NH_4OH) into 75 mL distilled water and stirred. The initial pH of the solution was about 10·5. Then, 2 g zinc acetate [$Zn(CH_3OO)_2.2H_2O$] powder was gradually added into the solution and stirred at room temperature until zinc acetate were completely solved resulting in a colourless precursor with pH of 9. Following this step, 1 g lead nitrate ($PbNO_3$) was added into the aforementioned solution while stirring, until pH reached 8. After dissolving the $Pb(NO_3)_2$ completely, NaOH solution of 1 mol was added into the above solution and stirred for 30 min. Ultimately, the pH of the solution reached 9·5. Then, 50 cc of the obtained solution was heated in microwave oven (EMS-820) for 5 min.

After microwave processing of the solution, the mixture was cooled to room temperature, resulting in a white precipitate. It was washed with deionised water and acetone several times to remove the impurities and residual materials. Then, it was dried in an oven at 60°C for 24 h and examined in terms of its structural and chemical.

Morphologies of the obtained powders were investigated by scanning electron microscopy (SEM, Philips XL30). The nanostructures of the synthesised materials were observed by transmission electron microscopy (FEG-TEM, Philips-CM200). The crystalline structure of the aforementioned powders was characterized by X-ray diffraction (XRD) analysis (Bruker D8 Discoverwith Cu K_α radiation (λ=1·54505 Å) and Bragg angle ranging from 5 to 80°. The composition, quality and molecular structure of the synthesised material were characterised by the Fourier transform infrared (FTIR, Bruker, Vector33) spectroscopy. The measurements were performed on the transmission mode in the mid-infrared range (500–4500 cm^{-1}) at the resolution of 4 cm^{-1}. The BET-N_2 measurements were performed using Micromeritics Gemini 2375equipment.

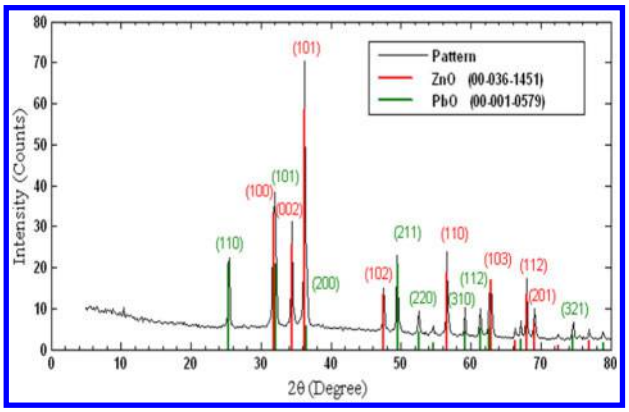

1 X-ray diffraction pattern of powder and identified phases

Results and discussion

X-ray diffraction was performed with Cu K_α radiation at tube parameters of 40 kV/40 mA using a Bruker D8. Discover XRD^2 micro-diffractometer equipped with the general area diffraction detection system (GADDS) and Hi-Star 2D area detector. The detector distance to the centre of diffraction was kept at 300 mm, which approximately covered the area of 20° in 2θ and 20° in χ with 0·02° resolution. In order to provide information from several grains in a single exposure, a large 0·8 mm X-ray beam size was selected and both in-plan oscillation and rotation were applied during the exposure. Four frames were collected and merged to cover the interval of 2θ from 5 to 80°. The exposure time was 300 s per frame. Merged frames were imported to the $DIFFRAC^{plus}$ EVA software for peak identification and phase analysis. Figure 1 shows the XRD pattern of synthesized powder using EVA software. Matching peaks with ICDD (International Center for Diffraction Data) database cards for different oxide phases were identified.

Hexagonal ZnO (36-1451) with cell constant of a=0·3248 Å and C=0·5206 Å is the majority phase. Other peaks were matched with Tetragonal Lead Oxide (01-0579). The sharp diffraction peak indicates that the produced composite has high crystallinity. Almost all peaks were identified by three oxide phases, indicating that pure powder was obtained. In fact, impurity level was less than a detectable level by X-ray diffraction. The average crystallite size of particles was determined by Scherrer formula as follows[36,37]

$$d = \frac{k\lambda}{D\cos(\theta)} \quad (1)$$

where d is the average crystallite size of powder, λ the wavelength of Cu K_α radiation (λ=1·54505 Å), D the full width at half maximum (FWHM) intensity of selected peak in degree, θ is the Bragg's diffraction angle and K is a constant usually equal to 0·9.[38] For each phase a certain peak was selected which was far enough from other peaks to be considered a single one. A Pearson VII function was implemented for curve fittings. The average crystallite size for ZnO was

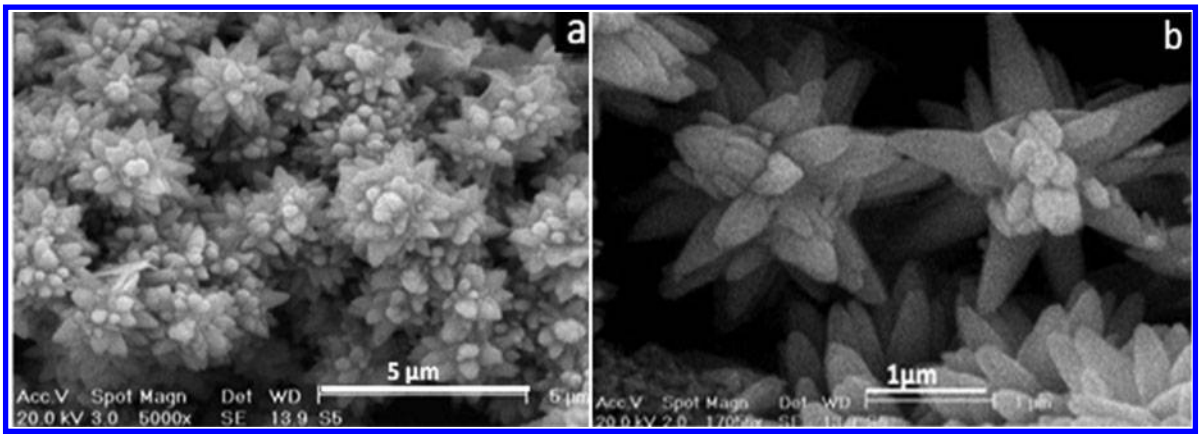

2 Images (SEM) of synthesised ZnO–PbO nanocomposite at two different magnifications

determined as 43·5 and 54·5 nm for PbO, using (002) and (110) peaks respectively.

In order to study of the attained nanopowder morphology, SEM features were utilised. Figure 2*a* displays the nanostructures of synthesised powder which is similar to cauliflower Fractal form. Indeed, nanostructures were designed as regular and well dispersive with a diameter in the range of 1–2·8 μm. The bigger magnification image was illustrated in Fig. 2*b*. It can also be observed that nanocomposite of ZnO–PbO were made of several sharp tip petals with a diameter in the range 300–500 nm and length of 600–1100 nm.

Transmission electron microscopy (TEM) was used to study the nanostructure morphology in more details and to support the SEM investigations as observed in Fig. 3. The Fig. 3*a* shows high magnification of TEM image obtained from an individual flower. The black colour is easy to detect, and the cauliflower Fractal–like nanostructure composed of 21 petals is also clearly observed. Moreover, all the petals were led to a central core (peduncle) with an average diameter of about 1570 nm. In order to do more exploration, detached petals were studied as well. Figure 3*b* shows the dimensions of a three petals with the average length and average diameter of 240 and 94 nm respectively. In addition, it is observed that petals have a sharp tip. The composition of the petal like nanostructure was analysed with the EDX-equipment on the FE-SEM. The EDAX analysis of the selected petal (green colour in Fig. 3*b*) showed that this area is mainly composed of zinc, lead and oxygen with quantities of weight percentage as 26·95, 44·8 and 13·09 respectively as observed in Fig. 3*c*. The peak displaying the Cu *K* irradiation is related to copper TEM grid which was used in the experiment (Fig. 3*c*).

The molecular structure and composition of nanopowder were explored through the FTIR spectroscopy (Fig. 4). It can be seen from the figure that the FTIR spectrum of synthesised nanocomposite was obtained in the range of 500–4500 cm^{-1}. The observations provide evidence for the presence of zinc oxide and lead oxide. The bands between 465–530 and 1633 cm^{-1} are related to Zn–O bands. It is also observed that Pb–O band is located at 714 cm^{-1}. The stretching mode of vibration in C=O is seen at 900 cm^{-1}. The peak at 1380 cm^{-1} is attributed to symmetric C–O band. The band at 1550 cm^{-1} is related to N–H band. There are peaks at 3271 and 3435 cm^{-1} which correspond to the band of C–H and O–H respectively.

Regarding the performed tests, the mechanism of ZnO–PbO nanocomposite formation can be explained in more details. At the first step, 75 cc H_2O was added to

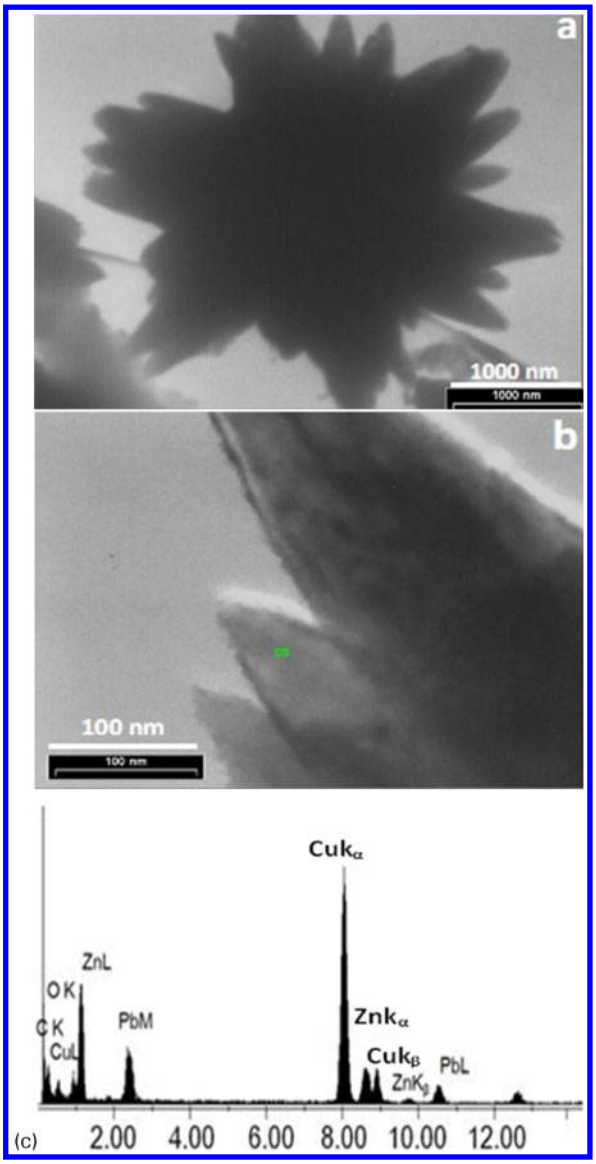

3 Images (TEM) of ZnO–PbO nanocomposits observing: *a* high magnification image of synthesised ZnO–PbO nanocomposite, *b* three petals and *c* EDAX of green point on one petal

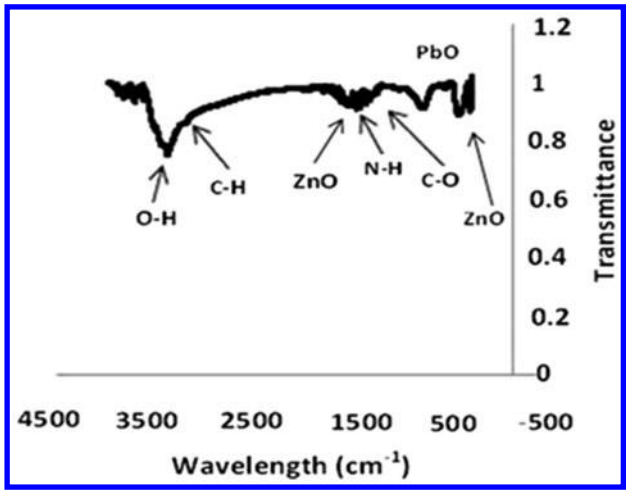

4 Typical FTIR spectrum of Zno–PbO nanocomposite

25 cc ammonium hydroxide to form a primary solution including NH_4^+ and OH^- ions as follows

$$NH_3(eq) + H_2O = NH_4^+ + OH^- \quad (2)$$

For the formation of zinc ammonium complexes, $[Zn(CH_3COO)_2.2H_2O]$ was added to the earlier solution. It significantly dissolves in the solution so that Zn^{2+} ions were made. Therefore, Zn^{2+} ions interact with NH_4^+ ions to form $Zn(NH_4)_2^{4+}$ as follows

$$Zn^{2+} + 2NH_4^+ = Zn(NH_4)_2^{4+} \quad (3)$$

Solution pH still remained in alkaline case, although released ions (e.g. $CHCOO^-$) can decrease solution pH. This phenomenon can be related to two factors. First, it may be induced by ammonium ions which makes complex agents and form complexes of zinc ammonium. Second, the presence of OH^- was derived from decomposition of NH_3(eq) could control the pH of the solution(equation 2) . Hence, the final solution had a trend to stay in alkaline case.

Previous studies have demonstrated that $Zn(NH_4)_2^{4+}$ complexes are more stable than $Zn(OH)_4^{2-}$ complexes at pH=9.[39] Therefore, most Zn ions tend to stay in $Zn(NH_4)_2^{4+}$ form at pH=9. Consequently, $Zn(OH)_4^{2-}$ ions act as an essential element for the formation of ZnO nuclei. According to literature, kinds of methods are utilised to fabricate lead oxide. Among them, PbO nanocrystals can be prepared by the thermal decomposition of $Pb(OH)_2$ at 180°C under P=1 at.[40] Here, in our investigation, lead nitrate and hydroxide sodium were used to make lead hydroxide as follows

$$Pb(NO_3)_2 + 2NaOH = Pb(OH)_2 + 2NaNO_3 \quad (4)$$

Under microwave irradiation, $Pb(OH)_2$ and $Zn(NH_4)_2^{4+}$ complexes creative PbO–ZnO primary nuclei. It can be illustrated by the equations following

$$Pb(OH)_2 \rightarrow PbO + H_2 \quad (5)$$

$$Zn(NH_4)_2^{4+} + 2(OH)^- \rightarrow ZNO + 2NH_4^+ + H_2O \quad (6)$$

The ZnO–PbO nanocomposite morphology architecture can be explicated in terms of the following reasons. Firstly, primary nuclei of ZnO–PbO were produced during microwave radiation and they were served as the primitive nucleation. Second, gathering of crystals make three-dimensional clusters which cause nucleation continuation and growth. Therefore, self-assembly of clusters seems to create a flower-like ZnO–PbO nanocomposite. Seemingly, growth process is not an easy method due to several reasons. It was found that intermolecular forces (e.g. Van der Waals) and ions absorption on the surfaces of nuclei have a great effect on the growth. Earlier researches indicate that ammonium ion is absorbed on the surfaces of acquired crystal due to high surface energy.[41] Thus, it is expected that ammonium ion can be effective on growth orientation of crystals.

In order to study the specific surface area and porous nature of the ZnO–PbO nanocomposite, a Brunauer–Emmett–Teller (BET) gas sorption measurement was performed. The BET specific surface area of the sample calculated from the N_2 isotherm at 77 K was found to be as high as about 150 $m^2\ g^{-1}$. Hence, the nanocomposite obtained here has an extremely high BET area, which is of great interest in catalysts, sensors and absorbents.

Conclusions

In situ ZnO–PbO nanocomposite was successfully synthesized for the first time using microwave method including several advantages, e.g. simplicity, high rate, low cost and easy access. In this study, zinc acetate $[Zn(CH_3OO)_2.2H_2O]$ and lead nitrate ($PbNO_3$) were respectively utilised as ZnO and PbO precursors in alkaline media derived from ammonium hydroxide (NH_4OH) and sodium hydroxide (NaOH). The morphology of the obtained nanocomposites is flower-like, which in petals have grown from all sides of peduncle with average length and average diameter of 175 and 375 nm respectively. Observation of as prepared material under EDAX test revealed that petals composed of zinc, lead and oxygen.

References

1. N. Liu, Y. Xu, H. Li, G. Li and L. Zhang: 'Effect of nano-micro TiN addition on the microstructure and mechanical properties of TiC based cermets', *J. Eur. Ceram. Soc.*, 2002, **22**, (13), 2409–2414.
2. N. Zanganeh, S. Zanganeh, A. Rajabi, M. Allahkarami, R. Rahbari Ghahnavyeh, A. Moghaddas, M. Aieneravaie and S. Sadrnezhaad: 'Flower-like boehmite nanostructure formation in two-steps', *J. Coord. Chem.*, 2014, doi: 10·1080/00958972·2014·892590.
3. E. Ekimov, E. Gromnitskaya, S. Gierlotka, W. Lojkowski, B. Palosz, A. Swiderska-Sroda, J. Kozubowski and A. Naletov: 'Mechanical behavior and microstructure of nanodiamond-based composite materials', *J. Mater. Sci. Lett.*, 2002, **21**, (21), 1699–1702.
4. J.-P. He, H.-M. Li, X.-Y. Wang and Y. Gao: 'In situ preparation of poly(ethylene terephthalate)–SiO2 nanocomposites', *Eur. Polym. J.*, 2006, **42**, (5), 1128–1134.
5. G. Gelinck, P. Heremans, K. Nomoto and T. D. Anthopoulos: 'Organic transistors in optical displays and microelectronic applications', *Adv. Mater.*, 2010, **22**, (34), 3778–3798.
6. H. Sadeghzadeh, A. Morsali, V. T. Yilmaz and O. Büyükgüngör: 'Synthesis of PbO nano-particles from a new one-dimensional lead (II) coordination polymer precursor', *Mater. Lett.*, 2010, **64**, (7), 810–813.
7. Y. W. Jun, J. S. Choi and J. Cheon: 'Shape control of semiconductor and metal oxide nanocrystals through nonhydrolytic colloidal routes', *Ang. Chem. Int. Ed.*, 2006, **45**, (21), 3414–3439.
8. G. Korotcenkov: 'Metal oxides for solid-state gas sensors: what determines our choice?', *Mater. Sci. Eng. B*, 2007, **139B**, (1), 1–23.
9. X. Wang, S. M. Tabakman and H. Dai: 'Atomic layer deposition of metal oxides on pristine and functionalized graphene', *J. Am. Chem. Soc.*, 2008, **130**, (26), 8152–8153.
10. M. Fernández-García, A. Martinez-Arias, A. Fuerte and J. Conesa: 'Nanostructured Ti-W mixed-metal oxides: structural and electronic properties', *J. Phys. Chem. B*, 2005, **109B**, (13), 6075–6083.

11. M. Mamak, N. Coombs and G. Ozin: 'Self-assembling solid oxide fuel cell materials: Mesoporous yttria-zirconia and metal-yttria-zirconia solid solutions', *J. Am. Chem. Soc.*, 2000, **122**, (37), 8932–8939.
12. Z. Yang and W. Xie: 'Soybean oil transesterification over zinc oxide modified with alkali earth metals', *Fuel Process. Technol.*, 2007, **88**, (6), 631–638.
13. E. Hosono, S. Fujihara, I. Honma and H. Zhou: 'The fabrication of an upright-standing zinc oxide nanosheet for use in dye-sensitized solar cells', *Adv. Mater.*, 2005, **17**, (17), 2091–2094.
14. A. Peiro, C. Domingo, J. Peral, X. Domenech, E. Vigil, M. Hernandez-Fenollosa, M. Mollar, B. Mari and J. Ayllon: 'Nanostructured zinc oxide films grown from microwave activated aqueous solutions', *Thin Solid Films*, 2005, **483**, (1), 79–83.
15. X. Cao, N. Wang, L. Wang and L. Guo: 'Porous ZnO nanobelts: synthesis, mechanism, and morphological evolutions', *J. Nanopart. Res.*, 2010, **12**, (1), 143–150.
16. E. Hosono, Y. Mitsui and H. Zhou: 'Metal-free organic dye sensitized solar cell based on perpendicular zinc oxide nanosheet thick films with high conversion efficiency', *Dalton Trans.*, 2008, (40), 5439–5441.
17. J. Chang, J. H. Lee, C. Najeeb, G. H. Nam, M. Lee and J. H. Kim: 'Area-selective growth of ZnO nanorod arrays on single-walled carbon nanotube patterns', *Scr. Mater.*, 2010, **63**, (5), 520–523.
18. Z. Jia and R. Misra: 'Tunable ZnO quantum dots for bioimaging: synthesis and photoluminescence', *Mater. Sci. Technol.*, 2013, **28**, (4), 221–227.
19. D. Depan and R. Misra: 'Structural and physicochemical aspects of silica encapsulated ZnO quantum dots with high quantum yield and their natural uptake in HeLa cells'. *J. Biomed. Mater. Res. A*, 2013, doi: 10·1002/jbm.a.34963.
20. R. D. Misra: 'Quantum dots for tumor-targeted drug delivery and cell imaging', *Nanomedicine*, 2008, **3**, (3), 271–274.
21. S. Chandrasekaran and R. Misra: 'Photonic antioxidant ZnS (Cd) nanorod synthesis for drug carrier and bioimaging', *Mater. Sci. Technol.*, 2013, **28**, (4), 228–233.
22. M. Salavati-Niasari, F. Mohandes and F. Davar: 'Preparation of PbO nanocrystals via decomposition of lead oxalate', *Polyhedron*, 2009, **28**, (11), 2263–2267.
23. S. McAllister, S. Patankar, I. F. Cheng and D. Edwards: 'Lead dioxide coated hollow glass microspheres as conductive additives for lead acid batteries', *Scr. Mater.*, 2009, **61**, (4), 375–378.
24. V. S. R. Raju, S. Murthy, F. Gao, Q. Lu and S. Komarneni: 'Microwave hydrothermal synthesis of nanosize PbO added Mg-Cu-Zn ferrites', *J. Mater. Sci.*, 2006, **41**, (5), 1475–1479.
25. M. Razavi, M. Rahimipour and A. Rajabi: 'Prenucleation effect on characterisations of synthesised nanocrystalline tungsten carbide via mechanical milling', *Mater. Technol. Adv. Perform. Mater.*, 2013, **28**, (3), 145–154.
26. H. Joel: 'Development and property evaluation of aluminum alloy reinforced with nano-ZrO2 metal matrix composites (NMMCs)', *Mater. Sci. Eng. A*, 2009, **A507**, (1–2), 110–113.
27. L. Torkian, M. Amini and E. Amereh: 'Sol-gel synthesised silver doped TiO 2 nanoparticles supported on NaX zeolite for photocatalytic applications', *Mater. Technol. Adv. Perform. Mater.*, 2013, **28**, (3), 111–116.
28. G. Arthi, J. Archana, M. Navaneethan, S. Ponnusamy, Y. Hayakawa and C. Muthamizhchelvan: 'Hydrothermal growth of ligand-passivated high surface area TiO_2 nanoparticles and dye-sensitized solar cell characteristics'. *Scr. Mater*., 2012, **68**, (6), 396–399.
29. M. Jazirehpour, H.-R. Bahahrvandi, A. Alizadeh and N. Ehsani: 'Facile synthesis of boron carbide elongated nanostructures via a simple in situ thermal evaporation process', *Ceram. Int.*, 2011, **37**, (3), 1055–1061.
30. H. Choi, H. Kim, S. Hwang, M. Kang, D. W. Jung and M. Jeon: 'Electrochemical electrodes of graphene-based carbon nanotubes grown by chemical vapor deposition', *Scr. Mater.*, 2011, **64**, (7), 601–604.
31. G.-N. He, B. Huang and H. Shen: 'Decisive role of Au layer on the oriented growth of ZnO nanorod arrays via a simple aqueous solution method', *J. Cryst. Growth*, 2010, **312**, (24), 3619–3624.
32. B. Pandey: 'Synthesis of zinc-based nanomaterials: a biological perspective', *Nanobiotechnol. IET*, 2012, **6**, (4), 144–148.
33. R. Feng, Y. Zhang, H. Li, D. Wu, X. Xin, S. Zhang, H. Yu, Q. Wei and B. Du: 'Ultrasensitive electrochemical immunosensor for zeranol detection based on signal amplification strategy of nanoporous gold films and nano–montmorillonite as labels'. *Anal. Chim. Acta*, 2013, **3**, (758), 72–79.
34. A. Kajbafvala, M. R. Shayegh, M. Mazloumi, S. Zanganeh, A. Lak, M. S. Mohajerani and S. K. Sadrnezhaad: 'Nanostructure sword-like ZnO wires: Rapid synthesis and characterization through a microwave-assisted route', *J. Alloys Compd*, 2009, **469**, (1–2), 293–297.
35. R. Nicula, M. Stir, K. Ishizaki, J. M. Català-Civera and S. Vaucher: 'Rapid nanocrystallization of soft-magnetic amorphous alloys using microwave induction heating', *Scr. Mater.*, 2009, **60**, (2), 120–123.
36. X. Liu, X. Song, C. Wei, Y. Gao and H. Wang: 'Quantitative characterization of the microstructure and properties of nanocrystalline WC–Co bulk', *Scr. Mater.*, 2012, **66**, (10), 825–828.
37. M. Bahgat, M. Khedr and M. Shaaban: 'Reduction of FeVO 4 to synthesise nanocrystalline ferrovanadium alloy', *Mater. Technol. Adv. Perform. Mater.*, 2008, **23**, (1), 13–18.
38. A. D. Krawitz: 'Introduction to diffraction in materials science and engineering', in 'Introduction to diffraction in materials science and engineering', (ed. A. D. Krawitz), Vol. 1, 424; 2001, New York, Wiley-VCH.
39. A. Kajbafvala, S. Zanganeh, E. Kajbafvala, H. R. Zargar, M. R. Bayati and S. K. Sadrnezhaad: 'Microwave-assisted synthesis of narcis-like zinc oxide nanostructures', *J. Alloys Compd*, 2010, **497**, (1–2), 325–329.
40. L. J. Chen, S. M. Zhang, Z. S. Wu, Z. J. Zhang and H. X. Dang: 'Preparation of PbS-type PbO nanocrystals in a room-temperature ionic liquid', *Mater. Lett.*, 2005, **59**, (24–25), 3119–3121.
41. L. Wang and M. Muhammed: 'Synthesis of zinc oxide nanoparticles with controlled morphology', *J. Mater. Chem.*, 1999, **9**, (11), 2871–2878.